Vaccine 39 (2021) 3862–3870

Contents lists available at ScienceDirect

Vaccine

journal homepage: www.elsevier.com/locate/vaccine

Single-dose combination nanovaccine induces both rapid and durable humoral immunity and toxin neutralizing antibody responses against *Bacillus anthracis*

Sean M. Kelly [a,d], Kristina R. Larsen [b,c], Ross Darling [b], Andrew C. Petersen [b], Bryan H. Bellaire [b,c,d], Michael J. Wannemuehler [b,d,*], Balaji Narasimhan [a,d,*]

[a] Department of Chemical and Biological Engineering, Iowa State University, Ames, IA, United States
[b] Department of Veterinary Microbiology and Preventive Medicine, Iowa State University, Ames, IA, United States
[c] Interdepartmental Microbiology Program, Iowa State University, Ames, IA, United States
[d] Nanovaccine Institute, Ames, IA, United States

ARTICLE INFO

Article history:
Received 8 February 2021
Received in revised form 24 April 2021
Accepted 23 May 2021
Available online 2 June 2021

Keywords:
Bacillus anthracis
Polyanhydride
Nanovaccine
Cyclic dinucleotide
Combination vaccine, neutralizing antibody

ABSTRACT

Bacillus anthracis, the causative agent of anthrax, continues to be a prominent biological warfare and bioterrorism threat. Vaccination is likely to remain the most effective and user-friendly public health measure to counter this threat in the foreseeable future. The commercially available AVA BioThrax vaccine has a number of shortcomings where improvement would lead to a more practical and effective vaccine for use in the case of an exposure event. Identification of more effective adjuvants and novel delivery platforms is necessary to improve not only the effectiveness of the anthrax vaccine, but also enhance its shelf stability and ease-of-use. Polyanhydride particles have proven to be an effective platform at adjuvanting the vaccine-associated adaptive immune response as well as enhancing stability of encapsulated antigens. Another class of adjuvants, the STING pathway-targeting cyclic dinucleotides, have proven to be uniquely effective at inducing a beneficial inflammatory response that leads to the rapid induction of high titer antibodies post-vaccination capable of providing protection against bacterial pathogens. In this work, we evaluate the individual contributions of cyclic di-GMP (CDG), polyanhydride nanoparticles, and a combination thereof towards inducing neutralizing antibody (nAb) against the secreted protective antigen (PA) from *B. anthracis*. Our results show that the combination nanovaccine elicited rapid, high titer, and neutralizing IgG anti-PA antibody following single dose immunization that persisted for at least 108 DPI.

1. Introduction

Bacillus anthracis is a Gram-positive, spore-forming bacteria that is the causative agent of the disease anthrax, whose spores are capable of lasting decades to centuries in the environment [1]. While natural inhalation infection of humans with *B. anthracis* spores is rare, the environmental stability of the spores and the high lethality of *B anthracis* make it capable of infecting hundreds of thousands of individuals with a single aerosol dispersion, making it a major biological warfare agent [2]. The difficulty in diagnosing anthrax, with its early onset of cold-like symptoms, is one of the major hurdles in managing the response to a widespread release of *B. anthracis* spores [2]. If anthrax infection is identified early after exposure, an extensive (60 days) therapeutic or prophylactic use of antibiotics is critical to prevent serious illness and death as spores can persist in vivo in a dormant state and cause disease well after the initial exposure [3]. In a mass exposure event, therapeutic intervention would require a largescale stockpile of antitoxins and antibiotics readily available at all times and would require that healthcare workers follow up with exposed individuals to patient compliance which is historically poor. For

Abbreviations: ASC, Antibody secreting cell; AUC, Area under the curve; AVA, Anthrax vaccine adsorbed; CDG, Cyclic di-GMP; CDN, Cyclic dinucleotide; CPH, 1,6-bis(*p*-carboxyphenoxy)hexane; CPTEG, 1,8-bis(*p*-carboxyphenoxy)-3,6-diaoctane; DPI, Days post-immunization; ED_{50}, Effective dose at 50% inhibition; EF, Edema factor; LF, Lethal factor; MFI, Mean fluorescence intensity; NO, Nitric oxide; NP, Nanoparticle; OVA, Ovalbumin; PA, Protective antigen; ROS, Reactive oxygen species; sPA, Soluble protective antigen; TLR, Toll-like receptor; TNA, Toxin neutralization assay.

* Corresponding authors at: Nanovaccine Institute, Ames, IA, United States.
E-mail addresses: mjwannem@iastate.edu (M.J. Wannemuehler), nbalaji@iastate.edu (B. Narasimhan).

https://doi.org/10.1016/j.vaccine.2021.05.077
0264-410X/

example, following the 2001 anthrax attack in the United States, fewer than half of the approximately 10,000 potentially exposed individuals completed the recommended 60 day course of antibiotic treatment [4].

Due to the limitations of these therapeutic interventions, as well as the propensity of dormant spores to persist in the lungs, pre- and post-exposure vaccination strategies are believed to be the most effective countermeasures against anthrax, where vaccination could generate protective immunity in exposed individuals before the onset of disease, as well as protect unexposed individuals against potential attack. Most vaccine strategies include the *B. anthracis* secretory factor protective antigen (PA), a component of the anthrax lethal toxin and edema toxin, when combined with lethal factor or edema factor, respectively. It is believed that neutralizing the ability of PA to heptamerize and translocate lethal factor (LF) and edema factor (EF) into the host cell cytosol is critical to prevent dissemination of the bacteria and toxemia associated with mortality [5]. A previous study demonstrated that anti-PA antibody titer and toxin neutralization titer following prime-boost vaccination correlated with protection in New Zealand white rabbits challenged intranasally with *B. anthracis* Ames strain spores [6]. In a similar study with guinea pigs, it was shown that anti-PA IgG antibody titer did not correlate with protection; however, toxin neutralization titer correlated with protection following prime-boost vaccination [7]. To further corroborate the importance of the humoral immune response in protection, a number of monoclonal antibodies have been generated that possess toxin neutralizing capacity [8], and there are reports of cross species modeling using ELISA and toxin neutralization assay data in multiple animal models to predict the efficacy of the Biothrax Anthrax Vaccine Adsorbed (AVA) vaccine in humans [9,10].

The current FDA-approved AVA vaccine consists of a cell-free, culture filtrate adsorbed to aluminum hydroxide. PA is believed to be the critical immunogenic component of the AVA vaccine as evidenced by the fact that anti-PA neutralizing antibodies are correlates of protection. However, there remains room for improvement to this vaccine formulation. First, it is a crude culture supernatant from *B. anthracis* strain V770-NP1-R that contains unquantified amounts of PA [11]. Second, prophylactic vaccination with AVA requires five administrations over 18 months, followed by annual boosters in order to maintain protective immunity. Third, the AVA vaccine is one of the most expensive pharmaceuticals being stored in the Strategic National Stockpile, owing to the refrigerated storage conditions as well as additional costs associated with cold chain distribution [12]. Therefore, it is sagacious/au fait to consider developing vaccines that can overcome shortcomings of the existing AVA vaccine including the ability to obviate the cold chain and be easily deployed in the event of exposure or outbreak event, all while providing both rapid and long-lasting protective immunity, ideally in a single dose.

Polyanhydride nanoparticle-based vaccines (i.e., nanovaccines) represent a promising platform that has proven effective against multiple bacterial and viral pathogens, including influenza [13], respiratory syncytial virus [14], and another biodefense pathogen *Yersinia pestis* [15]. Comprised of 1,6-bis(*p*-carboxyphenoxy) hexane (CPH) and 1,8-bis(*p*-carboxyphenoxy)-3,6-diaoctane (CPTEG), these copolymers are safe and induce mild inflammation at the site of injection [16]. Their hydrophobic properties enable sustained release of encapsulated payloads, which is tunable through varying copolymer composition [17], and can allow for dose-sparing through co-adjuvanting poorly immunogenic payloads [18]. In addition, polyanhydride nanoparticles demonstrate the ability to be stored without requiring refrigeration and can maintain the functional and antigenic stability of labile payloads [19,20]. For example, polyanhydride nanoparticles encapsulating PA were shown to release functionally active PA following four months of storage at 40 °C, while PA dramatically lost its bioactivity when similarly stored with Imject Alum [20]. Therefore, this nanovaccine platform shows promise both as an adjuvant as well as a shelf-stable delivery vehicle for PA-based vaccines.

Cyclic dinucleotides (CDNs) are a class of small molecules that function as universal secondary signaling molecules in bacterial and mammalian cells [21]. Recognition of CDNs through the STING (STimulator of INterferon Genes) pathway results in the induction of type I interferon (IFN), inducing anti-pathogenic activity [22]. Cyclic di-guanosine monophosphate (CDG), the most well-studied CDN to date, has potent adjuvant properties as vaccines adjuvanted with CDG induce a broad antibody response, characterized by the presence of multiple IgG subclasses in serum [23], and have been shown to elicit significantly higher antibody titers than alum-adjuvanted formulations [24]. Our previous work has demonstrated that immunization with chicken egg ovalbumin (Ova) adjuvanted with a synthetic analog of CDG in mice enhanced the antibody response within two weeks post-immunization compared to traditional TLR agonist-based adjuvants [25]. Mice immunized with PA adjuvanted with CDG had higher anti-PA IgG serum responses compared to animals immunized with the AVA vaccine, thereby making them an attractive adjuvant candidate to be included in future anthrax vaccines [25].

We have previously shown that a single dose of a combination nanovaccine comprising polyanhydride nanoparticles encapsulating the *Y. pestis* fusion protein F1-V co-adjuvanted with a non-canonical CDG adjuvant (containing 2′,5′-3′-5′ phosphate linkages) completely protected mice against pneumonic plague within 14 days post-immunization (DPI), while F1-V adjuvanted with CDG failed to provide complete protection [15]. Based on these results, we were interested in performing preliminary vaccination studies in mice to evaluate the immunogenicity of a single dose of shelf-stable 20:80 CPTEG:CPH polyanhydride nanoparticles encapsulating PA in combination with CDG to elicit rapid and durable anti-PA antibody responses, characterized by serum anti-PA IgG antibody titers and toxin neutralization ability following immunization.

2. Materials and methods

2.1. Materials

Chemicals used for polymer and nanoparticle synthesis: 4-*p*-hydroxybenzoic acid, tri-ethylene–glycol, 1,6-dibromohexane were obtained from Sigma Aldrich (St. Louis, MO); dimethyl formamide, acetic acid, acetonitrile, acetic anhydride, toluene, methylene chloride, pentane were purchased from Fisher Scientific (Fairlawn, NJ). 4-*p*-flourobenzonitrile was purchased from Apollo Scientific (Cheshire, UK). Dithio-R_P,R_P-cyclic di-guanosine monophosphate (R,R-Cyclic di-GMP (CDG)) was kindly provided by Aduro Biotech (Berkeley, CA).

2.2. Polymer synthesis

CPTEG and CPH monomers were first individually synthesized and melt polycondensation of the monomers was used to synthesize 20:80 CPTEG:CPH copolymer, as previously described [17,26]. Briefly, a 20:80 molar ratio of CPTEG:CPH diacids were added to acetic anhydride at a total mass concentration of 0.022 g/mL and allowed to react for 30 min at 125 °C. The solvent was subsequently removed by rotary evaporation, leaving a dry product which was then polymerized in an oil bath at 140 °C under vacuum (<0.1 torr) for six hours. The solid product was then dissolved in methylene chloride and precipitated in hexanes to yield the final copolymer product. Copolymers were dissolved into deuterated

chloroform for purity and molecular weight characterization via ^{1}H nuclear magnetic resonance spectroscopy. Copolymer molecular weight was ca. 5.3 kDa.

2.3. Nanoparticle synthesis and antigen encapsulation efficiency

Polyanhydride nanoparticles encapsulating PA (BEI resources, Cat# NR-3780, Manassas, VA), from *B. anthracis,* were synthesized using flash nanoprecipitations of 20:80 CPTEG:CPH copolymer, as previously described [15].

To determine PA encapsulation efficiency, 1 mg of PA-containing nanoparticles were weighed into 1.5 mL microcentrifuge tubes and suspended in 500 μL of 40 mM NaOH buffer following approximately 30 s of sonication. Periodically, samples were centrifuged at 10,000 rcf for 10 min, and 400 μL of supernatants were collected and replaced with fresh solution. Released protein was quantified via a microbicinchoninic acid (microBCA) assay and the encapsulation efficiency of PA was calculated as the total amount of protein released from the nanoparticles divided by the amount of protein added during nanoparticle synthesis [27]. The resulting encapsulation efficiency was 68%, indicating that the actual percent loading of PA encapsulated within the nanoparticles was 6.8% (w/w), following synthesis, while aiming for 10% (w/w) loading.

Nanoparticle mean size and size distribution were determined using ImageJ (National Institutes of Health, Bethesda, MD) analysis of nanoparticle images taken using scanning electron microscopy (SEM; JEOL 840 A, JEOL Ltd., Tokyo, Japan).

2.4. Animals

Male and female A/J mice, as well as female BALB/c mice, between six and eight weeks of age were obtained from Jackson Laboratory (Bar Harbor, ME). All studies involving the use of animals were carried out in accordance with and approval from the Iowa State University Institutional Animal Care and Use Committee.

2.5. Vaccinations

Separate groups of 6–8 week old A/J and BALB/c mice were immunized subcutaneously (SC) with one of the following vaccine formulations: 1) 5 μg PA encapsulated in 73.5 μg of 20:80 CPTEG:CPH (6.8% wt/wt) nanoparticles (NP), 2) 5 μg soluble PA adjuvanted with 25 μg CDG (dithio-R_P,R_P-cyclic diguanosine monophosphate) (Aduro Biotech, Berkeley, CA) (CDN Vaccine), 3) a combination of 5 μg PA encapsulated in 73.5 μg of 20:80 CPTEG:CPH (6.8% wt/wt) nanoparticles adjuvanted with 25 μg CDN (Combination Nanovaccine), 4) 5 μg soluble PA alone (sPA), or 5) 5 μg soluble PA adsorbed to Alhydrogel (Alhydrogel; Invivogen, San Diego, CA). The Alhydrogel formulation was prepared as a 1:9 vol ratio (i.e., a 1:10 dilution) of Alhydrogel adjuvant 2% (10 mg/mL aluminum content) in phosphate buffered saline (PBS), per manufacturer's instructions. Each animal received 0.2 mg of aluminum content. Data from female A/J mice (n = 4 per group) and female BALB/c mice (n = 6 per group) are presented in Figure 2. Data from male A/J mice (n = 8 per group) are presented in Figure 3, 4 and 5.

2.6. Serum antibody responses and ELISA

In longitudinal antibody studies (Figure 2 and 3), the same mice were bled via the saphenous vein multiple times at the indicated time points, either 14, 28, 56, and 108 DPI (Figure 2), or 15, 30, 46, 88, and 103 DPI (Figure 3). Serum was collected and stored at −20 °C until used for analysis. Costar 3590 96-well EIA/RIA high binding plates (Corning, Corning NY) were coated with 100 μL of PA or F1-V (0.5 μg/mL in PBS) and incubated overnight at 4 °C. Plates were blocked using either 2% (w/v) Difco gelatin in PBS (0.05 M, pH 7.2) containing 0.05% Tween-20 (PBS-T) for 2 h at room temperature or 2.5% (w/v) powdered skim milk dissolved in PBS-T (pH 7.4), that had been incubated for 2 h at 56 °C to inactivate any endogenous phosphatase activity. After three washes using PBS-T, serum samples were titrated across the plate using two-fold serial dilutions, starting at 1:100 or 1:200, in PBS-T containing 1% (v/v) normal goat serum. Samples were incubated overnight at 4 °C. After three washes in PBS-T, an alkaline phosphatase conjugated goat anti-mouse IgG (H + L) secondary detection antibody (Cat# 115-005-003, Jackson ImmunoResearch, West Grove, PA) was diluted 1:1000, and 100 μL was added to the wells and allowed to incubate at room temperature for 2 h. Plates were washed three times with PBS-T and alkaline phosphatase substrate (Cat# BP2534, Fisher Scientific, Hampton, NH) was added at 1 mg/mL in buffer containing 50 mM sodium carbonate, 2 mM magnesium chloride, and sodium bicarbonate added to achieve a pH of 9.3. Color was allowed to develop for 30 min or 2 h and analyzed using a SpectraMax 190 (Molecular Devices, San Jose, CA) spectrophotometer at a wavelength of 405 nm.

2.7. Cell culture

J774A.1 cells were cultured and maintained at 37 °C under 5% CO_2 in DMEM (Cat #15–013-CV, Corning) medium supplemented with 100 U/mL penicillin and 100 μg/mL streptomycin, 2 mM glutamine, and 10% FBS (i.e., complete tissue culture medium).

2.8. Toxin neutralization assay

In order to assess neutralizing activity of serum from vaccinated mice, a J774A.1 cell based cytotoxicity assay was adapted from a previously described protocol [28]. Briefly, J774A.1 cells were seeded into 96-well flat bottom plates (Costar, Cat #3595) at a concentration of 4×10^4 cells/well and allowed to adhere for 18 h. Serially diluted serum samples were prepared in separate 96-well plates by beginning at a 1:50 or 1:100 dilution and serially diluting them across the plate with two-fold dilutions. The serum samples were then incubated for 30 min with PA and LF (BEI resources, Cat# NR-28544), at constant concentrations of 50 ng/mL and 40 ng/mL, respectively, and then added to the wells containing the J774A.1 cells. The cell-serum-toxin mixture was allowed to incubate for 4 h after which 25 μL of a 5 mg/mL solution of 3-[4,5-dimethylthiazol-2-yl]-2,5-diphenyltetrazolium bromide (MTT) reagent (Invitrogen, Cat# M6494, Carlsbad, CA) was added. After two hours of incubation, supernatants were removed and 100 μL of dimethyl sulfoxide (Fisher Scientific, Cat# D128-500) was added to lyse the cells and solubilize formazan crystals. The OD of each sample at 555 nm was measured using a SpectraMax 190 spectrophotometer.

The first two time points (15 and 46 DPI) were performed in the same assay. The final time point (103 DPI) was performed in a separate assay. Therefore, as an inter-assay control, a previous serum sample collected 46 DPI from a mouse immunized with the Combination Nanovaccine used in the toxin neutralization assay for 15 and 46 DPI time points was used in the assay for 103 DPI samples as well. The titration curves for this sample in both assays was similar, with ED_{50} values of 13,602 and 14,033, respectively, for both assays, indicating consistency in responses between experiments. In addition, each assay included the following controls: cells without toxin (OD > 2.0), cells incubated with toxin but without serum (OD < 0.25), and cells incubated with toxin plus pooled serum from mice pre-immunization (OD < 0.25).

2.9. Peptide microarray printing and analysis

102 linear peptides containing 13- to 20-mer amino acid sequences (10 or 11 amino acid overlaps) (BEI resources, Cat# NR-527) spanning the full length of PA antigen, as well as the full-length PA antigen, *Y. pestis* fusion protein F1-V, and OVA were printed onto Nexterion Slide AL (Schott, Louisville, KY) using a BioRobotics MicroGRID II microarray printer (Genomic Solutions, Inc. Ann Arbor, MI). Peptides and proteins were first dissolved in DMSO at 10 mg/mL to ensure dissolution, then diluted 10-fold in water to 1 mg/mL. The solution was diluted two-fold to bring the final concentration to 0.5 mg/mL in 1x print buffer (5% (v/v) DMSO, 137 mM NaCl, 9 mM KOH, 11.3 mM NaH_2PO_4). The full-length PA antigen was used as a positive control, while F1-V and OVA were used as irrelevant controls. Slides were printed with 16 arrays per slide, each array containing 7x15 spots per array, with peptides printed in a serpentine pattern in duplicate. Following printing, slides were vacuum sealed and stored at −80 °C until further use. The microarray assay and analysis was performed as previously described [15] using serum from PA-immunized mice collected at 15 and 88 DPI.

2.10. ELISPOT analysis of bone marrow and spleen

ELISPOT analysis was performed as previously described [15]; however, plates were coated overnight with 5 μg/mL PA in PBS prior to blocking with complete tissue culture medium.

2.11. Statistical analyses

Data generated from anti-PA serum IgG ELISA assays were Log2 transformed and analyzed within each time point via one-way ANOVA with a Tukey post-test for multiple comparisons. Results from the toxin neutralization experiments were analyzed by determining the inflection point of the antibody dilution curve reported as the effective dilution at 50% inhibition (ED_{50}) using nonlinear regression modeling on GraphPad Prism 8.0 (GraphPad Software, La Jolla, CA) and Log2 transformed. Toxin neutralization responses were also quantified by determining the mean area under the curve (AUC) for each treatment group. Differences in ED_{50} and AUC between treatment groups were determined via one-way ANOVA with a Tukey post-test for multiple comparison. For PA peptide microarray analysis, a Student's *t* test was used for comparison of background-corrected mean fluorescence intensity (MFI) of sera from vaccination groups for each peptide. Binding of serum antibodies to a peptide was considered detectable if the spot binding background-corrected MFI of serum from a vaccination group was significantly ($p \leq 0.05$) higher than that of serum from naïve animals (prior to immunization). For bone marrow and spleen ELISPOT analysis, statistical significance between groups was determined by Kruskal-Wallis and Mann-Whitney tests. Statistical analyses of the PA peptide microarray was performed using R v3.4.1. All other analyses were performed using GraphPad Prism 8.0 (GraphPad Software, La Jolla, CA).

3. Results

3.1. Polyanhydride nanovaccine characterization

The 6.8%-loaded PA (w/w) 20:80 CPTEG:CPH nanoparticles were characterized for size distribution and encapsulation efficiency of PA. The size of the nanoparticles was consistent with previous work [15], with a mean diameter of 255 ± 98 nm and a polydispersity index of 0.15 indicating a narrow size distribution (Figure 1). The encapsulation efficiency of the PA within the nanoparticles was 68%.

3.2. Combination nanovaccine elicits rapid anti-PA antibody responses that persisted for at least 108 DPI

To assess the ability of both CDNs and polyanhydride nanoparticles to elicit serum anti-PA IgG responses, female A/J mice (n = 4 per group) were immunized SC with a single dose of the vaccine formulations described in the Materials and Methods section. Serum samples were collected throughout 108 DPI and anti-PA IgG titers were determined. Mice immunized with each of the vaccine formulations attained anti-PA titers > 2^{15} after 28 days that were maintained for at least 108 DPI (Figure 2A). Sera from CDN Vaccine- or Combination Nanovaccine-vaccinated mice contained significantly ($p \leq 0.05$) higher anti-PA IgG antibodies that remained elevated for at least 56 days compared to mice immunized with sPA. A similar trend was also observed with female BALB/c mice (Figure 2B). At 108 DPI, sera of A/J mice immunized with the Combination Nanovaccine maintained titers of ~2^{18} that were significantly ($p \leq 0.05$) higher compared to that for animals immunized with sPA (e.g., ~2^{15}). The polyanhydride nanoparticle formulation (NP) alone was unable to rapidly enhance the magnitude of the anti-PA antibody titer. These results indicate that CDG was the primary contributor to the rapid anti-PA serum IgG responses and strongly suggests the need to include CDG co-adjuvant in the nanovaccine formulation.

Next, the ability of the Combination Nanovaccine to induce anti-PA antibody responses was compared to PA adjuvanted with alhydrogel. Male A/J mice (n = 8 per group) were immunized SC with a single dose of one of the following vaccine formulations: i) 5 μg soluble PA (sPA), ii) 5 μg soluble PA adjuvanted with alhydrogel (Alhydrogel; 1:9 vol ratio = 0.2 mg aluminum content per mouse), or iii) 5 μg PA encapsulated into polyanhydride nanoparticles co-adjuvanted with 25 μg CDG (Combination Nanovaccine). Beginning at 15 DPI, serum samples were collected over 103 days to assess the magnitude of the anti-PA antibody responses. Combination Nanovaccine and Alhydrogel formulations induced significantly ($p \leq 0.0001$) higher anti-PA total IgG antibody titers (~2^{13}) as early as 15 DPI compared to sPA (~2^{8}), and these titers increased to ~2^{15} and were maintained over the course of 103 DPI (Figure 3). There was no significant difference in the magnitude of the anti-PA IgG titers between mice vaccinated with the Combination Nanovaccine or Alhydrogel.

3.3. Combination nanovaccine elicits enhanced rapid toxin neutralization antibodies against PA

As the magnitude of the anti-PA serum IgG response was similar between the Combination Nanovaccine and Alhydrogel formulations, toxin neutralization assays were performed using a J774A.1 cell cytotoxicity assay and serum from mice vaccinated with either formulation, as described above. Interestingly, despite having similar titers of total anti-PA IgG at 15 DPI (Figure 3), sera from mice immunized with the Combination Nanovaccine had significantly ($p = 0.0078$) higher toxin neutralizing antibody responses compared to sera from mice immunized with the Alhydrogel formulation (Figure 4A and Figure Supplementary Fig. 1A and 1D). The ability of serum from Combination Nanovaccine-immunized mice to neutralize toxin—mediated cell death was similar to that of serum from the Alhydrogel formulation-immunized mice at 46 DPI and 103 DPI (Figure 4B and C and Figure Supplementary Fig. 1B–D). Serum collected at 103 DPI from Alhydrogel and Combination Nanovaccine-immunized mice did not have significantly higher toxin neutralization capabilities compared to serum from sPA-immunized mice when comparing ED_{50} values, however, these

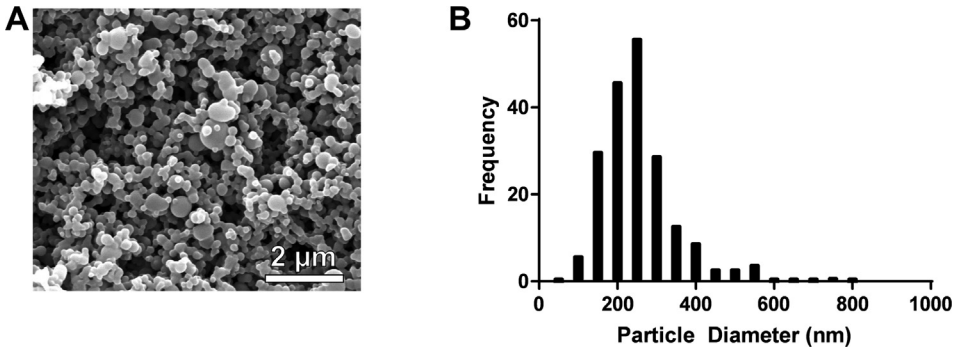

Fig. 1. Characterization of PA Nanovaccine. (A) Representative scanning electron micrograph image of PA nanovaccine (scale bar = 2 μm). Nanoparticle mean diameter was 255 ± 98 nm, determined via ImageJ analysis. (B) Size distribution of 6.8% (w/w) PA 20:80 CPTEG:CPH nanoparticles (255 ± 98 nm), determined via ImageJ analysis.

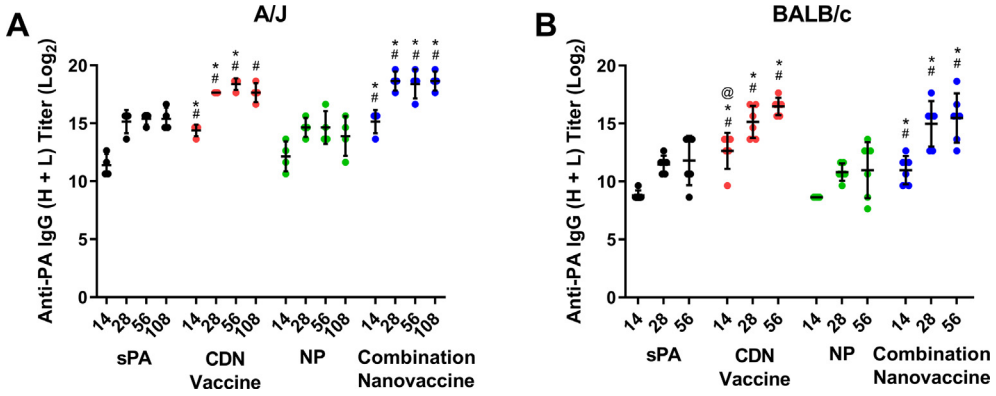

Fig. 2. Combination Nanovaccine induces rapid and long-lived antibodies against protective antigen. Either (A) female A/J mice (n = 4 per group) or (B) female BALB/c mice (n = 6 per group) were vaccinated SC with PA adjuvanted in different vaccine formulations. The formulations consisted of 5 μg PA encapsulated in 20:80 CPTEG:CPH nanoparticles (NP), 5 μg soluble PA adjuvanted with 25 μg CDNs (CDN Vaccine), a combination nanovaccine comprising of 5 μg PA encapsulated in 20:80 CPTEG:CPH nanoparticles adjuvanted with 25 μg CDN (Combination Nanovaccine), or 5 μg soluble PA alone (sPA). Total serum IgG (H + L) antibody titer to PA was quantified via ELISA at 14, 28, 56, and 108 DPI. Titer values were Log2 transformed and compared at each time point for statistical significance between vaccination groups via an ordinary one-way ANOVA with a Tukey's multiple comparison test. P value is indicated as follows for each comparison indicated (*#@$ = $p \leq 0.05$) (# vs NP, $ vs CDN Vaccine, @ vs Combination Nanovaccine, * vs sPA). Individual animals are shown with bars indicating mean ± SD.

were significantly ($p \leq 0.05$) different when comparing AUC (Figure Supplementary Fig. 1C and D).

3.4. Anti-PA IgG responses to linear epitopes in sera from vaccinated animals

To further characterize the quality of the anti-PA antibody response, a linearly overlapping peptide array was used to assess the ability of serum antibodies to bind to linear peptides spanning the full length of PA. A detectable response was defined as having significantly ($p \leq 0.05$) higher anti-PA antibody binding (measured by MFI) compared to naïve serum samples.

Serum from immunized mice was analyzed at 15 and 88 DPI to assess differences between early antibody responses induced by the vaccine formulations, where there were significant differences in anti-PA neutralizing antibody titers (Figure 4A), and later, when the anti-PA IgG neutralizing titers were similar (Figure 4C). At both time points, serum from mice immunized with sPA, Alhydrogel + PA, and the Combination Nanovaccine formulation demonstrated binding to intact PA (see row labeled 'PA'), whereas the naïve controls did not (Figure Supplementary Fig. 2). Serum IgG from vaccinated mice did not bind to OVA; however, serum from animals vaccinated with the PA-specific Combination Nanovaccine demonstrated binding to F1-V at both 15 and 88 DPI, which was not observed with any of the other vaccine formulations. This was confirmed after performing ELISA using serum collected at 46 DPI, in which serum from Combination Nanovaccine-immunized mice had significantly ($p \leq 0.05$) higher anti-F1-V IgG antibodies compared to mice immunized with either Alhydrogel or sPA vaccine formulations (Figure Supplementary Fig. 3).

At 15 DPI, there was no detectable antibody response to any peptides in mice vaccinated with sPA or PA adjuvanted with alhydrogel (Supplementary Figs. 2A and C). However, serum from mice vaccinated with the Combination Nanovaccine demonstrated significantly ($p < 0.05$) higher anti-PA IgG responses to peptides 13, 17, 18, 19, 24, 34, 38, 101, and 102 compared to naïve controls. By 88 DPI, serum responses from sPA-immunized mice still did not bind significantly to any linear peptides; however, serum from Alhydrogel-immunized animals had significantly ($p < 0.05$) higher anti-PA IgG responses to peptides 13 and 18 over naïve controls. Serum from Combination Nanovaccine-immunized animals showed significantly ($p < 0.05$) higher anti-PA IgG responses to peptide 101.

3.5. Combination nanovaccine induces long-lived antibody secreting cells in bone marrow and spleen

As the magnitude of the serum anti-PA IgG response between mice immunized with the Combination Nanovaccine and Alhydrogel were similar and persisted for 103 DPI, it was hypothesized that the maintenance of the long-lived serum anti-PA IgG response was due to the presence of long-lived antibody secreting cells (ASCs) residing in the bone marrow and spleen of immunized mice. To test this, ELISPOT analysis of bone marrow and spleen

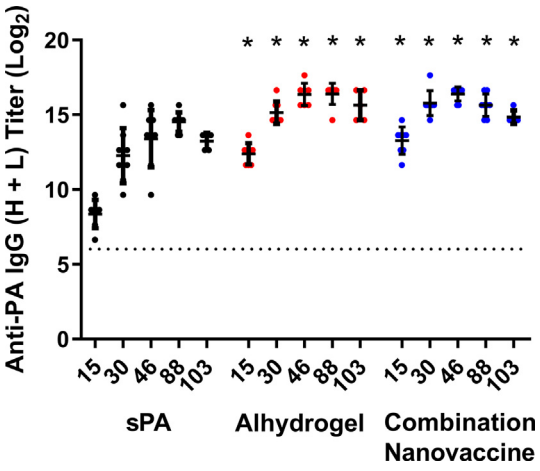

Fig. 3. Combination Nanovaccine elicits rapid and long-lived antibodies against protective antigen. Male A/J mice (n = 8 per group) were vaccinated SC with PA adjuvanted in different vaccine formulations. The formulations consisted of 5 μg soluble PA adsorbed to a 1:9 dilution of alhydrogel (Alhydrogel), a combination of 5 μg PA encapsulated in 20:80 CPTEG:CPH nanoparticles adjuvanted with 25 μg CDN (Combination Nanovaccine), or 5 μg soluble PA alone (sPA). Total serum IgG (H + L) antibody titer to PA was quantified via ELISA at 15, 30, 46, 88, and 103 DPI. Titer values were Log2 transformed and compared at each time point for statistical significance between vaccination groups via an ordinary one-way ANOVA with a Tukey's multiple comparison test. * $p \leq 0.05$ compared to sPA. Individual animals are shown with bars indicating mean ± SD. The dashed line represents the average anti-PA IgG (H + L) antibody titer from naïve animals prior to immunization.

homogenates from immunized mice collected at 103 DPI was performed. The analysis revealed that bone marrow of mice immunized with sPA did not have significantly more PA-specific ASCs when compared to naïve controls (Figure 5A). In contrast, there were significantly ($p \leq 0.05$) higher numbers of PA-specific ASCs in bone marrows of mice immunized with either the Combination Nanovaccine or Alhydrogel. The Alhydrogel formulation induced significantly ($p \leq 0.05$) higher PA-specific ASCs in bone marrow compared to the Combination Nanovaccine. Interestingly, in the spleen, only mice immunized with the Combination Nanovaccine had significantly ($p \leq 0.05$) higher numbers of PA-specific ASCs compared to naïve controls and higher than sPA and Alhydrogel formulations (Figure 5B).

4. Discussion

B. anthracis is a highly virulent pathogen, capable of infecting hundreds of thousands of individuals with a single aerosol dispersion of spores, making it a significant biological warfare agent [2]. Vaccination is likely to be the most cost effective and patient-friendly option to prevent disease following exposure of civilians and war fighters to *B. anthracis*. The major issues that need to be resolved in next generation anti-PA vaccines are: i) reducing the number of doses required to effectively induce high titer neutralizing antibody; ii) identification and selection of adjuvants that promote antibody responses to neutralizing rather than non-neutralizing epitopes; and iii) improving the shelf-life stability of the formulated vaccines [11,29,30]. In this work, we designed a combination nanovaccine composed of polyanhydride nanoparticles encapsulating PA co-adjuvanted with CDNs and assessed its ability to induce anti-PA neutralizing IgG responses following a single immunization. The motivation for using the combination adjuvant approach is predicated upon the previously described immunostimulatory capabilities of both adjuvants [15], in addition to the shelf stability provided by the polyanhydride nanoparticles [19,20].

In this work, preliminary vaccination studies evaluating the immune response of female A/J mice demonstrated that inclusion of CDNs as a co-adjuvant, either alone or combined with the NP formulation, led to significant increases in serum anti-PA IgG titers throughout 108 DPI compared to NP alone (Figure 2). These results are in agreement with our recently published work showing that a combination of CDNs with a polyanhydride nanovaccine encapsulating the *Y. pestis* fusion protein F1-V led to an increase in magnitude of serum anti-F1-V IgG titers [15].

As the manifestation of anthrax infection following intranasal exposure can occur rapidly [31], it is critical to develop vaccines that can rapidly enhance anti-PA antibody responses which, in conjunction with antimicrobials, can best protect individuals with suspected or known exposure to *B. anthracis* [32]. As protection against lethal *B. anthracis* challenge appears to correlate with serum IgG toxin neutralization capacity [6,7], development of vaccines that can induce anti-PA toxin neutralizing antibodies is thought to be beneficial to enhancing protection against a possible exposure event. Similar to immune responses induced by PA adjuvanted with alhydrogel, the Combination Nanovaccine

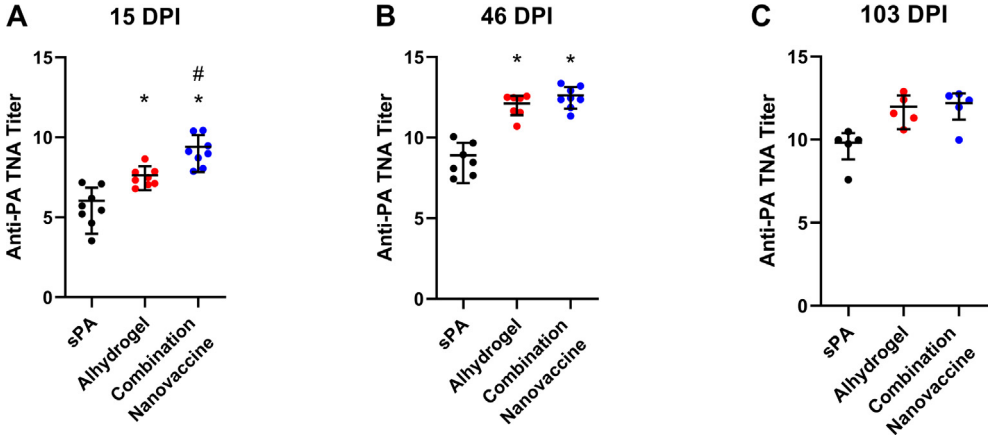

Fig. 4. Combination Nanovaccine elicits rapid and long-lived toxin neutralizing antibodies against the protective antigen. Male A/J mice (n = 8 per group) were vaccinated SC with PA adjuvanted in different vaccine formulations. The formulations consisted of 5 μg soluble PA adsorbed to a 1:9 dilution of alhydrogel (Alhydrogel), a combination of 5 μg PA encapsulated in 20:80 CPTEG:CPH nanoparticles adjuvanted with 25 μg CDN (Combination Nanovaccine), or 5 μg soluble PA alone (sPA). Neutralizing antibody titers were determined in serum collected (A) 15, (B) 46, and (C) 103 DPI using a J774A.1 cell-based MTT cytotoxicity assay as described in Materials and Methods. Titer values were determined as the inflection point of the antibody dilution curve reported as the effective dilution at 50% inhibition (ED_{50}) and were Log2 transformed and compared at each time point for statistical significance between treatment groups via an ordinary one-way ANOVA with a Tukey's multiple comparison test. * $p \leq 0.05$ compared to sPA. # $p \leq 0.05$ compared to Alhydrogel. Individual animals are shown with bars indicating mean ± SD.

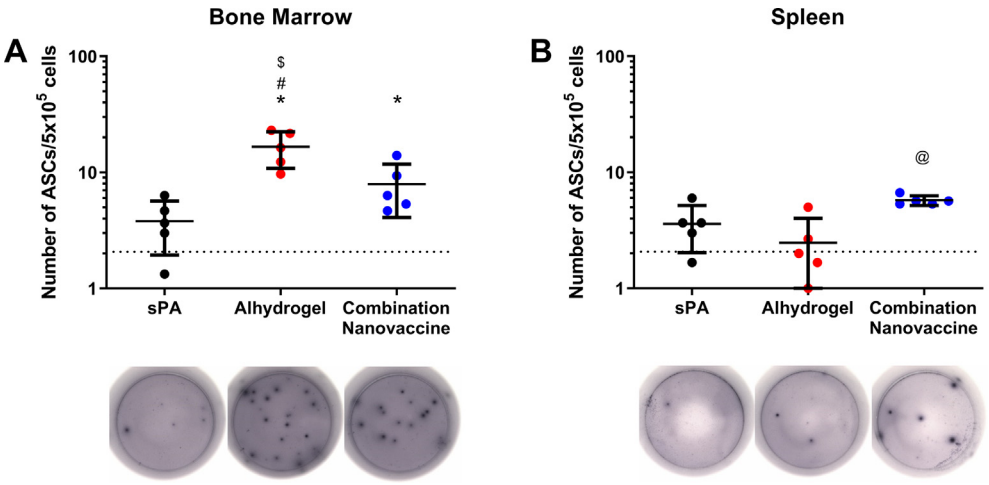

Fig. 5. Combination Nanovaccine induces long-lived anti-PA antibody secreting cells in both bone marrow and spleen. Male A/J mice (n = 8 per group) were vaccinated SC with PA adjuvanted in different vaccine formulations. The formulations consisted of 5 μg soluble PA adsorbed to a 1:9 dilution of alhydrogel (Alhydrogel), a combination of 5 μg PA encapsulated in 20:80 CPTEG:CPH nanoparticles adjuvanted with 25 μg CDN (Combination Nanovaccine), or 5 μg soluble PA alone (sPA). Bone marrow and splenic lymphocytes were harvested at 103 DPI from groups of immunized or naïve mice (n = 5 per group), and were analyzed via ELISPOT for the number of PA-specific IgG-secreting antibody secreting cells (ASCs). Data represent the number of PA-specific IgG-secreting ASCs per 500,000 cells in either (A) bone marrow or (B) spleen from individual mice. The dashed line represents the number of non-specific (i.e., naturally occurring) ASCs per 500,000 cells determined from naïve mice. Statistical significance between groups was determined by Kruskal-Wallis and Mann-Whitney tests. * represents $p \leq 0.05$ compared to naïve mice. # represents $p \leq 0.05$ compared to sPA-immunized mice. $ represents $p \leq 0.05$ compared to Combination Nanovaccine. @ represents $p \leq 0.05$ compared to naïve, sPA, and Alhydrogel formulations. Individual animals are shown with bars indicating mean ± SD.

induced a rapid, high titer anti-PA IgG antibody response by 15 DPI that was maintained for 103 DPI (Figure 3). When the toxin neutralizing abilities of serum were evaluated, however, the Combination Nanovaccine elicited higher toxin neutralizing antibody titers compared to PA adjuvanted with alhydrogel at 15 DPI (Figure 4A and Figure Supplementary Fig. 1A and D). This capability of CDN-containing vaccines to induce rapid toxin neutralizing IgG could lead to rapid post-exposure prophylaxis immunity for individuals in an acutely affected area. Rapid generation of neutralizing antibodies may also have the potential of reducing the number of vaccine doses needed to achieve protective immunity in an outbreak scenario where there may be fewer vaccine doses available than necessary, as well as reducing the recommended 60 days of antibiotic treatment when potential exposure has occurred. These considerations are currently being evaluated for emergency preparedness against a large-scale, aerosol release event by the Centers for Disease Control [32].

The potent antibody responses induced by activating the STING pathway with CDNs are reportedly capable of inducing significantly higher antibody titers to antigens than those induced when adjuvanted with alum [15,24,33], including the AVA vaccine [25]. In this study, the overall serum IgG production to PA was similar between the Combination Nanovaccine and Alhydrogel formulations through 103 DPI; however, the serum anti-PA neutralizing response induced by the Combination Nanovaccine was significantly elevated 15 DPI (Figure 4A). This is hypothesized to be due to lower expression levels of nitric oxide (NO) and reactive oxygen species (ROS) by antigen presenting cells stimulated by CDNs, when compared to TLR agonists [25]. In particular, increased NO and ROS expression levels are known to deleteriously affect both innate and adaptive immunity, including altering innate cell function [34], B cell survival and subsequent antibody production, lower levels of BAFF production [35–37], and lymphatic vessel function [38]. Although the exact mechanism(s) of action of alum adjuvants is still being investigated, one likely mechanism is through NLRP3 inflammasome activation [39,40], due to alum-induced generation of ROS [40–42]. Therefore, we posit that the observed early increase in serum anti-PA neutralizing responses with the Combination Nanovaccine compared to that induced by the Alhydrogel-based vaccine may be mediated by the lower levels of NO and ROS induced by CDNs.

Numerous neutralizing monoclonal antibodies against PA have been documented against every domain of the PA antigen, with the majority of these antibodies being directed at the furin cleavage domain (Domain 1; peptides 3–39), endosomal pore formation domain (Domain 2; peptides 38–70 and Domain 3; peptides 69–84), and receptor binding domains (Domain 4; peptides 83–102) [43]. The most well-studied monoclonal antibody, 14B7 and its affinity-matured variants, are known to bind PA conformational epitopes on domain 4 [44–47]. However, monoclonal antibodies have also been reported to bind linear epitopes on domain 1 [48] and domain 4 [49]. Following microarray analysis of PA linear peptides, it was observed that there was an overall low detectable response of serum IgG from both Combination Nanovaccine- and Alhydrogel-immunized mice to linear peptides spanning the full length PA antigen; however, serum from Combination Nanovaccine-immunized mice was able to bind to peptides 13, 17, 18, 19, 24, 34, 38 (Domain 1), as well as 101 and 102 (Domain 4) by 15 DPI, while there was no detectable antibody responses to any peptides by serum from Alhydrogel-immunized mice at that time point (Figure Supplementary Fig. 2). Considering the apparent low detectable response by serum IgG collected at 15 and 88 DPI from mice vaccinated with any vaccine, juxtaposed with the observed increase in toxin neutralization capabilities at 46 and 103 DPI in Combination Nanovaccine- and Alhydrogel-immunized sera compared to sPA, we hypothesize that the majority of the antibodies induced by both vaccines is to conformational epitopes on PA but warrants further investigation.

The maintenance of long-lived antibody responses are believed to derive from long-lived plasma cells residing in bone marrow, secondary lymph organs, and gut, which can persist for decades, and secrete large quantities of antibodies, including IgG, IgM, and IgA [50,51]. In this work, PA-specific IgG-ASCs were detected at 103 DPI in the bone marrow and spleen of mice immunized with the Combination Nanovaccine, but only in bone marrows of mice immunized with the Alhydrogel formulation (Figure 5). The pres-

ence of PA-specific ASCs in bone marrow are in agreement with previous work from our laboratories, where F1-V-specific IgG-ASCs from combination nanovaccine-immunized mice were detected in bone marrow 215 DPI; however, F1-V-specific ASCs were not detected in spleen [15]. Therefore, the Combination Nanovaccine was able to induce long-lived anti-PA serum IgG responses that derived, at least in part, from PA-specific ASCs residing in both bone marrow and spleen.

In conclusion, a combination nanovaccine comprising polyanhydride nanoparticles co-adjuvanted with CDNs was able to elicit both rapid and durable anti-PA IgG antibody responses that were characterized by significantly higher serum anti-PA toxin neutralizing antibody responses by 15 DPI compared to PA adjuvanted with alhydrogel. Altogether, these preliminary results lay the foundation for the further platform development and testing of shelf-stable polyanhydride-based anthrax nanovaccines that can provide both rapid and durable immunity to bolster biodefense preparedness.

Declaration of Competing Interest

Balaji Narasimhan and Michael Wannemuehler are co-founders of ImmunoNanoMed Inc., a start-up with business interests in the development of nano-based vaccines against infectious diseases. Narasimhan also has a financial interest in Degimflex LLC, a start-up with business interests in the development of flexible degradable electronic films for biomedical applications.

Acknowledgements

The authors thank Drs. David Kanne, Chudi Ndubaku, and Thomas Dubensky, Jr at Aduro Biotech for providing the CDG used for in vivo experiments. The authors also thank Dr. Chris Minion at Iowa State University for providing the BioRobotics MicroGRID II printer used for printing microarray slides.

Funding

This work was supported by the NIH-NIAID (R01 AI111466) and the Iowa State University Nanovaccine Institute. B.N. acknowledges the support of the Vlasta Klima Balloun Faculty Chair.

Author contributions

SMK, KLR, RJD, MJW, and BN contributed to conception and design of the studies. SMK, KLR, and RJD contributed to performing vaccination studies and in vitro assays. SMK, KLR, RJD, and ACP contributed to analysis of the experiments. SMK, KLR, RJD, MJW, and BN contributed to drafting, revising, and approval of the final version of the manuscript.

Appendix A. Supplementary material

Supplementary data to this article can be found online at https://doi.org/10.1016/j.vaccine.2021.05.077.

References

[1] Dragon DC, Rennie RP. The ecology of anthrax spores: tough but not invincible. Can Vet J = La Rev Vet Can 1995;36(5):295–301.
[2] WHO. Anthrax in humans and animals. World Organ Anim Heal 2008;219.
[3] Kaur M, Singh S, Bhatnagar R. Anthrax vaccines: present status and future prospects. Expert Rev Vaccines 2013;12(8):955–70. https://doi.org/10.1586/14760584.2013.814860.
[4] Shepard CW, Soriano-Gabarro M, Zell ER, Hayslett J, Lukacs S, Goldstein S, et al. Antimicrobial postexposure prophylaxis for anthrax: adverse events and adherence. Emerg Infect Dis 2002;8(10):1124–32. https://doi.org/10.3201/eid0810.020349.
[5] Moayeri M, Leppla SH, Vrentas C, Pomerantsev AP, Liu S. Anthrax pathogenesis. Annu Rev Microbiol 2015;69(1):185–208. https://doi.org/10.1146/annurev-micro-091014-104523.
[6] Little SF, Ivins BE, Fellows PF, Pitt MLM, Norris SLW, Andrews GP. Defining a serological correlate of protection in rabbits for a recombinant anthrax vaccine. Vaccine 2004;22(3–4):422–30. https://doi.org/10.1016/j.vaccine.2003.07.004.
[7] Chun J-H, Choi O-J, Cho M-H, Hong K-J, Seong WK, Oh H-B, et al. Serological correlate of protection in guinea pigs for a recombinant protective antigen anthrax vaccine produced from *Bacillus* Brevis. Osong Public Heal Res Perspect 2012;3(3):170–6. https://doi.org/10.1016/j.phrp.2012.07.006.
[8] Lee K, Hwang S, Paik DJ, Kim WK, Kim JM, Youn J. *Bacillus*-derived poly-γ-glutamic acid reciprocally regulates the differentiation of T helper 17 and regulatory T cells and attenuates experimental autoimmune encephalomyelitis. Clin Exp Immunol 2012;170(1):66–76. https://doi.org/10.1111/j.1365-2249.2012.04637.x.
[9] Fay MP, Follmann DA, Lynn F, Schiffer JM, Stark G, Kohberge R, et al. Anthrax vaccine induced antibodies provide cross-species prediction of survival to aerosol challenge. Sci Transl Med 2012;4(151):151–1126. https://doi.org/10.1126/scitranslmed.3004073.
[10] Stark GV, Sivko GS, Vanraden M, Schiffer J, Taylor KL, Hewitt JA, et al. Cross-species prediction of human survival probabilities for accelerated anthrax vaccine absorbed (AVA) regimens and the potential for vaccine and antibiotic dose sparing HHS public access. Vaccine 2016;34(51):6512–7. https://doi.org/10.1016/j.vaccine.2016.06.041.
[11] Kondakova OA, Nikitin NA, Evtushenko EA, Ryabchevskaya EM, Atabekov JG, Karpova OV. Expert review of vaccines vaccines against anthrax based on recombinant protective antigen: problems and solutions vaccines against anthrax based on recombinant protective antigen: problems and solutions; 2019. https://doi.org/10.1080/14760584.2019.1643242.
[12] Nicholson A, Wollek S, Kahn B, Herrmann J. In: Nicholson A, Wollek S, Kahn B, Herrmann J, editors. The Nation's Medical Countermeasure Stockpile. Washington, D.C.: National Academies Press; 2016. https://doi.org/10.17226/23532.
[13] Ross K, Senapati S, Alley J, Darling R, Goodman J, Jefferson M, et al. Single dose combination nanovaccine provides protection against influenza A virus in young and aged mice. Biomater Sci 2019;7(3):809–21. https://doi.org/10.1039/C8BM01443D.
[14] McGill JL, Kelly SM, Kumar P, Speckhart S, Haughney SL, Henningson J, et al. Efficacy of mucosal polyanhydride nanovaccine against respiratory syncytial virus infection in the neonatal calf. Sci Rep 2018;8(1):1–15. https://doi.org/10.1038/s41598-018-21292-2.
[15] Wagner DA, Kelly SM, Petersen AC, Peroutka-Bigus N, Darling RJ, Bellaire BH, et al. Single-dose combination nanovaccine induces both rapid and long-lived protection against pneumonic plague. Acta Biomater 2019;100:326–37. https://doi.org/10.1016/j.actbio.2019.10.016.
[16] Huntimer L, Ramer-Tait AE, Petersen LK, Ross KA, Walz KA, Wang C, et al. Evaluation of biocompatibility and administration site reactogenicity of polyanhydride-particle-based platform for vaccine delivery. Adv Healthc Mater 2013;2(2):369–78. https://doi.org/10.1002/adhm.201200181.
[17] Torres MP, Vogel BM, Narasimhan B, Mallapragada SK. Synthesis and characterization of novel polyanhydrides with tailored erosion mechanisms. J Biomed Mater Res - Part A 2006;76(1):102–10. https://doi.org/10.1002/jbm.a.30510.
[18] Huntimer L, Wilson Welder JH, Ross K, Carrillo-Conde B, Pruisner L, Wang C, et al. Single immunization with a suboptimal antigen dose encapsulated into polyanhydride microparticles promotes high titer and avid antibody responses. J Biomed Mater Res B Appl Biomater 2013;101(1):91–8. https://doi.org/10.1002/jbm.b.32820.
[19] Wagner-Muñiz DA, Haughney SL, Kelly SM, Wannemuehler MJ, Narasimhan B. Room temperature stable PspA-based nanovaccine induces protective immunity. Front Immunol 2018;9. https://doi.org/10.3389/fimmu.2018.00325.
[20] Petersen LK, Phanse Y, Ramer-Tait AE, Wannemuehler MJ, Narasimhan B. Amphiphilic polyanhydride nanoparticles stabilize *Bacillus anthracis* protective antigen. Mol Pharm 2012;9(4):874–82. https://doi.org/10.1021/mp2004059.
[21] Jenal U, Reinders A, Lori C. Cyclic Di-GMP: second messenger extraordinaire. Nat Rev Microbiol 2017;15(5):271–84. https://doi.org/10.1038/nrmicro.2016.190.
[22] Danilchanka O, Mekalanos JJ. Cyclic dinucleotides and the innate immune response. Cell 2013;154(5):962–70. https://doi.org/10.1016/j.cell.2013.08.014.
[23] Ebensen T, Schulze K, Riese P, Link C, Morr M, Guzmán CA. The bacterial second messenger cyclic DiGMP exhibits potent adjuvant properties. Vaccine 2007;25:1464–9. https://doi.org/10.1016/j.vaccine.2006.10.033.
[24] Hu D-L, Narita K, Hyodo M, Hayakawa Y, Nakane A, Karaolis DKR. C-Di-GMP as a vaccine adjuvant enhances protection against systemic methicillin-resistant *Staphylococcus aureus* (MRSA) infection. Vaccine 2009;27:4867–73. https://doi.org/10.1016/j.vaccine.2009.04.053.

[25] Darling RJ, Senapati S, Kelly SM, Kohut ML, Narasimhan B, Wannemuehler MJ. STING pathway stimulation results in a differentially activated innate immune phenotype associated with low nitric oxide and enhanced antibody titers in young and aged mice. Vaccine 2019;37(20). https://doi.org/10.1016/j.vaccine.2019.04.004.
[26] Kipper MJ, Wilson JH, Wannemuehler MJ, Narasimhan B. Single dose vaccine based on biodegradable polyanhydride microspheres can modulate immune response mechanism. J Biomed Mater Res - Part A 2006;76(4):798–810. https://doi.org/10.1002/jbm.a.30545.
[27] Wagner DA, Kelly SM, Petersen AC, Peroutka-Bigus N, Darling RJ, Bellaire BH, et al. Single-dose combination nanovaccine induces both rapid and long-lived protection against pneumonic plague. Acta Biomater 2019;100. https://doi.org/10.1016/j.actbio.2019.10.016.
[28] Ngundi MM, Meade BD, Lin TL, Tang WJ, Burns DL. Comparison of three anthrax toxin neutralization assays. Clin Vaccine Immunol 2010;17(6):895–903. https://doi.org/10.1128/CVI.00513-09.
[29] Verma A, Burns DL. Improving the stability of recombinant anthrax protective antigen vaccine. Vaccine 2018;36(43):6379–82. https://doi.org/10.1016/j.vaccine.2018.09.012.
[30] Oscherwitz J, Quinn CP, Cease KB. Anthrax vaccine recipients lack antibody against the loop neutralizing determinant: a protective neutralizing epitope from *Bacillus anthracis* protective antigen. Vaccine 2015;33(20):2342–6. https://doi.org/10.1016/j.vaccine.2015.03.037.
[31] Artenstein AW. Bioterrorism and biodefense. In: Infectious diseases, vol. 1. Elsevier; 2017. p. 670–679.e1. https://doi.org/10.1016/B978-0-7020-6285-8.00075-7.
[32] Bower WA, Schiffer J, Atmar RL, Keitel WA, Friedlander AM, Liu L, et al. Use of Anthrax Vaccine in the United States: Recommendations of the Advisory Committee on Immunization Practices, 2019. MMWR Recomm Reports 2019;68(4):1–14. https://doi.org/10.15585/mmwr.rr6804a1.
[33] Ogunniyi AD, Paton JC, Kirby AC, McCullers JA, Cook J, Hyodo M, et al. C-Di-GMP is an effective immunomodulator and vaccine adjuvant against pneumococcal infection. Vaccine 2008;26(36):4676–85. https://doi.org/10.1016/j.vaccine.2008.06.099.
[34] Serbina NV, Salazar-Mather TP, Biron CA, Kuziel WA, Pamer EG. TNF/INOS-producing dendritic cells mediate innate immune defense against bacterial infection. Immunity 2003;19(1):59–70. https://doi.org/10.1016/S1074-7613(03)00171-7.
[35] Sammicheli S, Kuka M, Di Lucia P, De Oya NJ, De Giovanni M, Fioravanti J, et al. Inflammatory monocytes hinder antiviral B cell responses. Sci Immunol 2016;1(4). https://doi.org/10.1126/sciimmunol.aah6789.
[36] Shah HB, Joshi SK, Rampuria P, Devera TS, Lang GA, Stohl W, et al. BAFF- and APRIL-dependent maintenance of antibody titers after immunization with T-dependent antigen and CD1d-binding ligand. J Immunol 2013;191(3):1154–63. https://doi.org/10.4049/jimmunol.1300263.
[37] Giordano D, Draves KE, Li C, Hohl TM, Clark EA. Nitric oxide regulates BAFF expression and T cell-independent antibody responses. J Immunol 2014;193(3):1110–20. https://doi.org/10.4049/jimmunol.1303158.
[38] Schmid-Schonbein GW. Nitric Oxide (NO) side of lymphatic flow and immune surveillance. Proc Natl Acad Sci 2012;109(1):3–4. https://doi.org/10.1073/pnas.1117710109.
[39] HogenEsch H, O'Hagan DT, Fox CB. Optimizing the utilization of aluminum adjuvants in vaccines: you might just get what you want. npj Vaccines 2018;3(1):51. https://doi.org/10.1038/s41541-018-0089-x.
[40] Wen Y, Shi Y. Alum: an old dog with new tricks. Emerg Microbes Infect 2016;5(1):1–5. https://doi.org/10.1038/emi.2016.40.
[41] Rathinam VAK, Vanaja SK, Fitzgerald KA. Regulation of inflammasome signaling. Nat Immunol 2012;13(4):333–1332. https://doi.org/10.1038/ni.2237.
[42] Ruwona TB, Xu H, Li X, Taylor AN, Shi Y, Cui Z. Toward understanding the mechanism underlying the strong adjuvant activity of aluminum salt nanoparticles. Vaccine 2016;34(27):3059–67. https://doi.org/10.1016/j.vaccine.2016.04.081.
[43] McComb RC, Martchenko M. Neutralizing antibody and functional mapping of *Bacillus anthracis* protective antigen—the first step toward a rationally designed anthrax vaccine. Vaccine 2016;34(1):13–9. https://doi.org/10.1016/j.vaccine.2015.11.025.
[44] Little SF, Leppla SH, Cora E. Production and characterization of monoclonal antibodies to the protective antigen component of *Bacillus anthracis* toxin. Infect Immun 1988;56(7):1807–13.
[45] Little SF, Novak JM, Lowe JR, Leppla SH, Singh Y, Klimpel KR, et al. Characterization of lethal factor binding and cell receptor binding domains of protective antigen of *Bacillus anthracis* using monoclonal antibodies. Microbiology 1996;142(3):707–15. https://doi.org/10.1099/13500872-142-3-707.
[46] Maynard JA, Maassen CBM, Leppla SH, Brasky K, Patterson JL, Iverson BL, et al. Protection against anthrax toxin by recombinant antibody fragments correlates with antigen affinity. Nat Biotechnol 2002;20(6):597–601. https://doi.org/10.1038/nbt0602-597.
[47] Harvey BR, Georgiou G, Hayhurst A, Jeong KJ, Iverson BL, Rogers GK. Anchored periplasmic expression, a versatile technology for the isolation of high-affinity antibodies from *Escherichia coli*-expressed libraries. Proc Natl Acad Sci 2004;101(25):9193–8. https://doi.org/10.1073/pnas.0400187101.
[48] Abboud N, De Jesus M, Nakouzi A, Cordero RJB, Pujato M, Fiser A, et al. Identification of linear epitopes in *Bacillus anthracis* protective antigen bound by neutralizing antibodies. J Biol Chem 2009;284(37):25077–86. https://doi.org/10.1074/jbc.M109.022061.
[49] Kelly-Cirino CD, Mantis NJ. Neutralizing monoclonal antibodies directed against defined linear epitopes on domain 4 of anthrax protective antigen. Infect Immun 2009;77(11):4859–67. https://doi.org/10.1128/IAI.00117-09.
[50] Brynjolfsson SF, Persson Berg L, Olsen Ekerhult T, Rimkute I, Wick M-J, Mårtensson I-L, et al. Long-lived plasma cells in mice and men. Front Immunol 2018;9(Nov):1–7. https://doi.org/10.3389/fimmu.2018.02673.
[51] Lightman SM, Utley A, Lee KP. Survival of long-lived plasma cells (LLPC): piecing together the puzzle. Front Immunol 2019;10(May):1–12. https://doi.org/10.3389/fimmu.2019.00965.